

## Harmonic generation by relativistic electrons during irradiance of a solid target by a short-pulse ultraintense laser

Wei Yu,<sup>1,2</sup> M. Y. Yu,<sup>1</sup> J. Zhang,<sup>3</sup> and Z. Xu<sup>2</sup>

<sup>1</sup>*Institut für Theoretische Physik I, Ruhr-Universität Bochum, D-44780 Bochum, Germany*

<sup>2</sup>*Shanghai Institute of Optics and Fine Mechanics, Shanghai 201800, People's Republic of China*

<sup>3</sup>*Department of Physics, University of Oxford, Oxford OX1 3PU, United Kingdom*

(Received 20 June 1997)

A simple surface current model is proposed for studying harmonic generation by a short-pulse high-intensity circularly polarized laser irradiating a solid target normally. Exact relativistic electron dynamics is taken into account. It is found that high harmonics peaked at directions normal to that of incidence are efficiently generated. [S1063-651X(98)50203-6]

PACS number(s): 52.40.Nk, 42.65.Ky, 41.60.Ap, 52.75.Ms

Recent advances in high-intensity laser technology and applications of coherent ultrashort-wavelength radiation have led to renewed interest in the generation of harmonics from laser interactions with plasmas [1–10]. In contrast to electron sources such as beams and storage rings, plasmas can provide large numbers of free electrons required for efficient interaction with the laser field. When the interaction is sufficiently nonlinear because of the intensity of the laser and/or processes in the plasma, harmonics of high order in the scattered radiation can be produced. In particular, the strongly relativistic electron quiver motion in an ultraintense ( $I\lambda^2 > 10^{18}$  W  $\mu\text{m}^{-2}$  cm<sup>2</sup>) laser can lead to high harmonics. Since for longer-pulse lasers and/or lower density plasmas, the relativistic nonlinearities are to the lowest order canceled by the ponderomotive reaction of the plasma [7], it is of interest to investigate harmonic generation by the highly relativistic free electrons during the interaction of an ultrashort, ultraintense laser with a solid density plasma.

In a recent experiment [9,10] solid targets were irradiated obliquely by a short-pulse (<0.4 ps) linearly polarized laser at intensities in excess of  $10^{19}$  W/cm<sup>2</sup>. Contrary to expectation [1,2], high harmonics (up to the 68th) in nonspecular directions and with large ( $> 10^{-6}$ ) conversion efficiencies were observed. For fixed laser intensities at lower values ( $\leq 7 \times 10^{18}$  W/cm<sup>2</sup>), the conversion efficiency decreases rapidly with the harmonic number, whereas for high ( $\geq 10^{19}$  W/cm<sup>2</sup>) intensities this decrease is less pronounced and tend to flatten at high ( $\geq 50$ ) harmonic numbers. The results are similar for *s* and *p* polarized laser lights. Some of these features qualitatively agree with those found from a one-dimensional particle-in-cell simulation of Gibbon [8]. The wide angular spread of the high harmonics was attributed to rippling of the interaction surface [9].

In this paper we consider harmonic generation by relativistic surface currents during *normal* irradiance of a solid target by a short-pulse ultraintense *circularly* polarized laser. Exact relativistic electron dynamics is taken into account, assuming that the target is not significantly altered by the laser [2–6]. It is found that although most of the incident energy is backscattered at the fundamental frequency, higher harmonics appear as the laser intensity increases. The angle corresponding to strongest scattering for each harmonic in-

creases with the harmonic number. The angular spread around this brightest angle, broad for the lower harmonics, decreases with the harmonic number. For high harmonic modes both the angle and its spread are peaked in a direction nearly perpendicular to the incident light.

The radiated power per unit solid angle of the *n*th harmonic from a current source  $\vec{j}$  consisting of say, electrons moving relativistically in the circularly polarized laser field, can be expressed in general as [11]

$$\frac{dP_n}{d\Omega} = \frac{n^2 \omega_0^2}{8\pi^3 c^3} \left| \int d^3x e^{-ink_0 \hat{v} \cdot \vec{x}} \int_0^{2\pi} d\tau \vec{G}_n \right|^2, \quad (1)$$

where  $\vec{G}_n \equiv \hat{v} \times (\hat{v} \times \vec{j}) \exp[in(\tau - k_0 \hat{v} \cdot \vec{\Delta})]$ , and  $\hat{v} = (1, \theta, \phi)$  is the observation direction,  $\vec{x}$  is the coordinate vector of the source at, say  $\tau = 0$ ,  $\vec{\Delta}(\vec{x}, \tau) = \int_0^\tau \vec{v}(\vec{x}, \tau') d\tau'$  is its displacement,  $\tau = \omega_0 t$ ,  $k_0 = \omega_0/c$ , and  $\omega_0$  is the laser frequency. That is,  $\vec{x} + \vec{\Delta}$  is the instantaneous location of the source [12]. The formula (1) can be derived from the Maxwell equations, the only assumption being that the observer be far from the source.

For simplicity we neglect laser energy absorption by the plasma. We also assume uniform irradiance within the focal spot, whose radius *a* is much larger than the laser wavelength. Thus, we have  $\vec{j}(\vec{x}, t) = \vec{j}(z, t)$  and  $\vec{\Delta}(\vec{x}, t) = \vec{\Delta}(z, t)$ , and Eq. (1) can be rewritten as

$$\frac{dP_n}{d\Omega} = \frac{a^2}{2\pi c} F_n(\theta) \left| \int dz e^{-ink_0 \cos\theta z} \int_0^{2\pi} d\tau \vec{G}_n \right|^2, \quad (2)$$

where we have introduced the factor

$$F_n(\theta) = \left( \frac{nk_0}{2\pi a} \right)^2 \left| \int_0^a d\rho \rho \int_0^{2\pi} d\varphi e^{-ink_0 \rho \sin\theta \cos(\varphi - \phi)} \right|^2 \\ = [J_1(nk_0 a \sin\theta) / \sin\theta]^2, \quad (3)$$

which is often used in optics in connection to diffraction from a circular hole. For  $k_0 a \gg 1$ ,  $F_n(\theta)$  peaks sharply at  $\theta = 0$  and oscillates with increasing angle, as is shown in Fig. 1 for  $n = 1$  and  $k_0 a = 100$ .

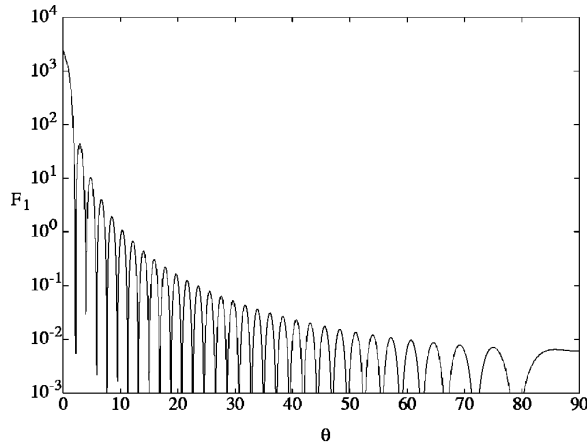


FIG. 1. The variation of dimensionless diffraction factor  $F_n(\theta)$ , for  $n=1$  and  $k_0 a=100$ .

In the low-intensity limit, the electron displacement in the laser field is much less than the laser wavelength ( $k_0 \Delta \ll 1$ ), and does not significantly affect the radiation. The time integral in Eq. (2) can then be expressed explicitly in terms of the  $n$ th Fourier component  $\vec{j}_n = (1/2\pi) \int d\tau \vec{j} \exp(in\tau)$  of the current density. One obtains

$$\frac{dP_n}{d\Omega} = \frac{2\pi a^2}{c} F_n(\theta) \left| \int dz \hat{v} \times (\hat{v} \times \vec{j}_n) e^{-ink_0 \cos\theta z} \right|^2 \quad (4)$$

for the radiated power in the  $n$ th harmonic. The generation of a harmonic can thus be understood in terms of  $\vec{j}_n$ . That is, the  $n$ th current component  $\vec{j}_n$  acts as the source for the  $n$ th harmonic. In this case all harmonics are in the specular direction (with respect to the incident light). On the other hand, in the relativistic regime the factor  $k_0 \hat{v} \cdot \vec{\Delta}$  in  $\vec{G}_n$  becomes important since the electron displacement is now comparable to the laser wavelength. It follows that the time integral in Eq. (2) can no longer be expressed in terms of a simple Fourier component of the current density. Clearly, the finite displacement can significantly change the angle of harmonic radiation [13].

For irradiance by an ultrashort, ultraintense laser, the hydrodynamic response of the laser-produced plasma does not play a major role. During the short time of interaction the plasma does not have time to expand significantly. Instead of the appearance of a large inhomogeneous corona, the density profile remains steplike, which can be modeled by a solid-density plasma filling a half-space. That is, the plasma density is  $n_0$  for  $z \geq 0$  and zero for  $z < 0$ . At the vacuum-plasma interface, the boundary condition is  $H_i(0,t) = 2H_t(0,t)$ , where  $H_i$  and  $H_t$  are the magnetic fields of the incident and transmitted modes, respectively. In the limit  $n_0 \rightarrow \infty$  the transmitted mode can be replaced by a surface current  $j_s(t)$ . The boundary condition [11] is then  $(4\pi/c)j_s(t) = 2H_t(0,t)$ . In the solid density plasma considered here we have  $n_0 \gg n_c$ , where  $n_c$  is the critical density, the penetration of the laser radiation is confined to an extremely small (usually less than one tenth the laser wavelength) region on the target surface. Thus, in Eq. (2) one can set  $\vec{j}(z,t) \sim \vec{j}(t)\delta(z)$ , where  $\vec{j}(t) = (m\omega_0 c^2/2\pi e)\gamma\vec{\beta}(t)$ ,  $\gamma = (1$

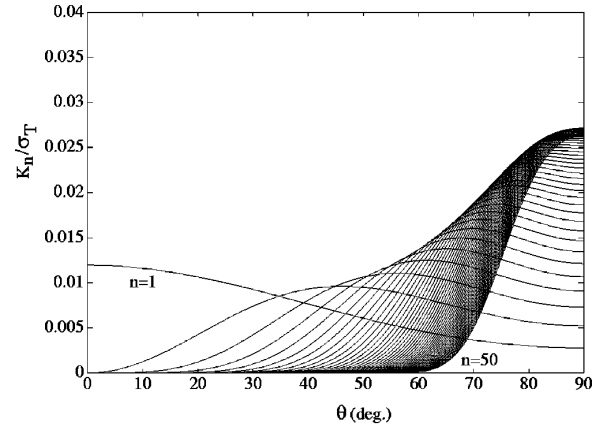


FIG. 2. The variation of the dimensionless quantity  $K_n(\theta)/\sigma_T$ , which describes the radiation from a single electron, for  $n=1$  to 50, and  $q=3$ .

$-\beta^2)^{-1/2}$ ,  $\vec{\beta} = \vec{v}/c$ , and  $\vec{v}$  is the electron quiver velocity in the incident circularly polarized laser field.

Harmonic emission can be considered as nonlinear scattering of light, and described in terms of the differential cross section for light scattered per unit solid angle at the  $n$ th harmonic, or

$$\frac{d\sigma_n}{d\Omega} = \frac{1}{I} \frac{dP_n}{d\Omega} = \frac{3c\sigma_T}{2e^2\omega_0^2 q^2} \frac{dP_n}{d\Omega},$$

where  $\sigma_T$  is the Thomson cross section,  $I = (c/4\pi)|E_i|^2$  is the laser intensity and  $q = e|E_i|/m\omega_0 c = 1.2 \times 10^{-9} \sqrt{I\lambda^2}$  (where  $I$  and  $\lambda$  are in units of  $\text{W}/\text{cm}^2$  and  $\mu\text{m}$ , respectively) is the laser strength parameter. For laser scattering from a solid target we have then

$$\frac{d\sigma_n}{d\Omega} = (8\pi a^2/3n^2\sigma_T)\gamma^2 F_n(\theta) K_n(\theta), \quad (5)$$

where the radiation  $K_n(\theta)$  from a single electron quivering (rotating) in the incident laser field is [11,13]

$$\begin{aligned} K_n(\theta) &= \frac{3n^2\sigma_T}{16\pi^3 q^2} \left| \int_0^{2\pi} d\tau \hat{v} \times (\hat{v} \times \vec{\beta}) e^{in(\tau - k_0 \hat{v} \cdot \vec{\Delta})} \right|^2 \\ &= \frac{3n^2\sigma_T}{4\pi q^2} [\cotan^2 \theta J_n^2(n\beta \sin\theta) + \beta^2 J_n'^2(n\beta \sin\theta)], \end{aligned} \quad (6)$$

where  $\vec{\beta} = \beta(\cos\hat{\pi} + \sin\hat{\tau})$  and  $\beta = q/\sqrt{1+q^2}$ . Note that  $K_n(\theta)$  depicts the strong radiation from a single electron, while the diffraction term  $F_n(\theta)$  takes into account the collective effect of all the electrons participating in the motion [11].

Figure 2 shows the angular dependence of  $K_n(\theta)$  for the first to the 50th (from left to right) harmonics for  $q=3$  (or  $I\lambda^2 \sim 1 \times 10^{19} \text{ W cm}^{-2} \mu\text{m}^2$ ). One sees that in the nonlinear scattering from a single relativistic electron, a considerable part of the scattered energy is in the higher harmonics. Scattering at the fundamental laser frequency is comparatively weak, although it still peaks at the normal of the electron orbit. With increasing harmonic order, the angular distribu-

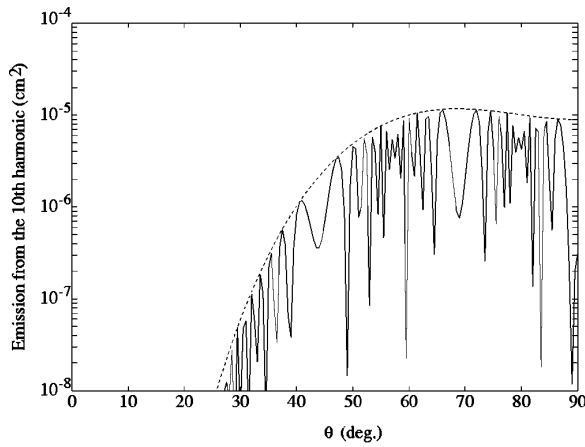


FIG. 3. The differential cross section (in  $\text{cm}^2$ ) of the 10th harmonic scattered from a solid-density plasma, with  $q=3$  and  $k_0a=100$ . The dashed lines represent the envelope calculated from the asymptotic expression (8).

tion of the harmonics is tipped forward towards the plane of the electron orbit, together with increasingly sharper peaks. The radiation at the higher harmonics is folded into a sharp cone centered on the orbit plane, an effect that results directly from the relativistic displacement  $\Delta$  of the electron in the laser field. It is worth noting that with its acceleration being perpendicular to the velocity, an electron moving in a circularly polarized laser field radiates more effectively than that in a comparable linearly polarized field, and the radiation spectrum will therefore contain more harmonic components than that of linearly polarized lights [11].

The total nonlinear scattering from a solid-density plasma can be calculated by taking into account the diffraction factor  $F_n(\theta)$ . Since both  $K_1(\theta)$  and  $F_1(\theta)$  peak at  $\theta=0$ , the power at the fundamental frequency is much enhanced in the direct backscattering direction. The scattering efficiency  $\eta_n = \sigma_n / \pi a^2$  is then

$$\eta_1 = \frac{4}{\beta^2} \int [\cotan^2 \theta J_1^2 + \beta^2 J_1'^2] F_1(\theta) \sin \theta d\theta, \quad (7)$$

where the argument of the Bessel functions is  $\beta \sin \theta$ . Since  $\eta_1$  is close to unity, most of the incident laser energy is mirror reflected at the same frequency.

For the harmonics, however, the peaks of  $K_n(\theta)$  and  $F_n(\theta)$  are not matched. As a result, the harmonics deviate from the backscattering direction and appear at larger angles. Figures 3 and 4 show for  $q=3$  and  $k_0a=100$  the angular distribution of the 10th and 50th harmonics, respectively. Because of the diffraction factor  $F_n(\theta)$ , the resulting differential cross section oscillates with the scattering angle  $\theta$ . These oscillations, with a period roughly of the order  $\sin^{-1}(\lambda/na)$ , are at present too fine structured to be measured experimentally. The upper envelope of the oscillations, with  $F_n(\theta)$  in the limit  $nk_0a \sin \theta \gg 1$ , namely,

$$F_n(\theta) \sim \frac{2 \cos^2(nk_0a \sin \theta + \varphi)}{\pi nk_0a \sin^3 \theta} \rightarrow \frac{2}{\pi nk_0a \sin^3 \theta}, \quad (8)$$

is shown as dashed lines in Figs. 3 and 4. Thus, while the lower harmonics have a relatively wide angular spread, the

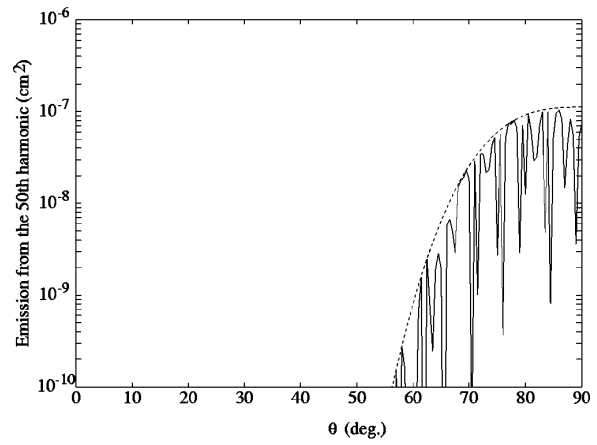


FIG. 4. Same as Fig. 3, but for the 50th harmonic.

high harmonics tend to appear at angles nearly perpendicular to the incident laser. Obviously there is no forward scattering in the present model.

From Eqs. (5) and (8), the conversion efficiency of the  $n$ th harmonic is

$$\eta_n \sim \frac{8}{n \pi k_0 a \beta^2} \int [\cotan^2 \theta J_n^2 + \beta^2 J_n'^2] \frac{d\theta}{\sin^2 \theta}, \quad (9)$$

where the argument of the Bessel functions is  $n\beta \sin \theta$ . The efficiencies are shown in Fig. 5 for  $n=10$  and 50 as a function of the laser strength parameter  $q$ . There is a threshold for the appearance of any harmonic component. Above the threshold the harmonic appears and its conversion efficiency increases rapidly with  $q$  until a certain value, and thereafter it seems to flatten out. In Fig. 6, the conversion efficiency versus the harmonic number for  $q=5$  (or  $I\lambda^2 \sim 4 \times 10^{19} \text{ W cm}^{-2} \mu\text{m}^2$ ) is shown.

We have used a simple surface current model to consider the scattering of a short-pulse high-intensity laser off a solid target. The surface current approach is applicable since in the present model, namely, normal incidence of a circularly polarized laser in the absence of plasma response, the target electrons do not execute axial motion. That is, the target remains steplike [2–6,13]. In real situations, the target can deform somewhat by possible laser prepulse or rise-time ef-

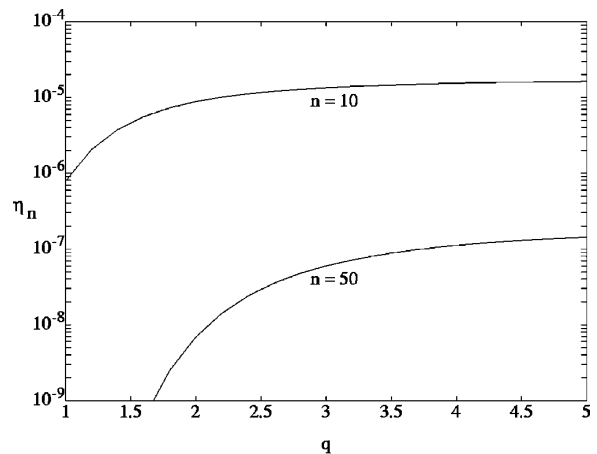


FIG. 5. The conversion efficiencies of the 10th and 50th harmonics vs  $q$ .

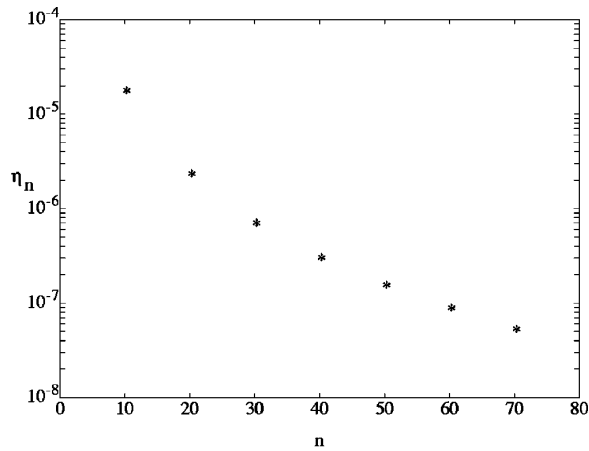


FIG. 6. The conversion efficiency vs the harmonic number for  $q=5$ .

facts, and a corona can appear in front of it. Our results show that high harmonics can appear in the scattered light. Each harmonic has a lower angular cutoff, with the dominating fundamental harmonic mostly backscattered. The lower harmonics have a wide angular spread from the cutoff angle up to the target plane, whereas the angular distribution becomes narrower and closer to the latter for the higher harmonics. The angular spread of the harmonics is due to the combined effects of light diffraction and large (within the laser period) electron displacement. The latter contribution is similar, but in a predictable manner, to that from target-surface rippling. It is also found that at fixed laser intensities of lower values

( $\leq 7 \times 10^{18}$  W/cm<sup>2</sup>), the conversion efficiency decreases rapidly with the harmonic number. For higher ( $\geq 10^{19}$  W/cm<sup>2</sup>) intensities, the decrease is not as pronounced and tend to flatten at high ( $\geq 50$ ) harmonic numbers.

Because of the simplifying assumptions made here, such as circular polarization of the laser, normal incidence, step-like target profile, etc., it is not strictly appropriate to compare our results with that of Norreys *et al.* [9,14]. Nevertheless, it is obvious from the formulation that the main mechanism proposed, namely, the contribution of the relativistic displacement  $\vec{\Delta}$ , should be universal for other polarizations and incidence angles. In this sense it is not surprising that the results here agree fairly well with those of Norreys *et al.* [9] in several general as well as unique features such as the angular spread, the scaling of the scattering efficiency, etc. The conversion efficiency obtained here for the high harmonics is about an order of magnitude lower than that of Norreys *et al.* [9], who however assumed isotropic radiation. In fact, because of the existence of an axial electron orbit component for oblique incidence and noncircular polarization, one expects that the corresponding angular spread of the scatter harmonics will be more isotropic than the case here. On the other hand, we note that the angular concentration predicted here for the high harmonics from the scattering of *circularly* polarized lights can be especially useful in many applications.

This work was supported by the Sonderforschungsbereich 191 Niedertemperatur Plasmen. W.Y. would like to thank the K. C. Wong Education Foundation and the Deutscher Akademischer Austauschdienst for support.

- 
- [1] R. L. Carman, C. K. Rhodes, and R. F. Benjamin, *Phys. Rev. A* **24**, 2649 (1981).
- [2] B. Besserides, R. D. Jones, and D. W. Forslund, *Phys. Rev. Lett.* **49**, 202 (1982).
- [3] P. Sprangle, E. Esarey, and A. Ting, *Phys. Rev. A* **41**, 4463 (1990).
- [4] E. Esarey, A. Ting, P. Sprangle, and D. Umstadter, *IEEE Trans. Plasma Sci.* **21**, 95 (1993).
- [5] S. C. Wilks, W. L. Kruer, and W. B. Mori, *IEEE Trans. Plasma Sci.* **21**, 120 (1993).
- [6] E. Esarey, S. K. Ride, and P. Sprangle, *Phys. Rev. E* **48**, 3003 (1993).
- [7] See, for example, W. B. Mori, *Phys. Scr.* **T52**, 28 (1994).
- [8] P. Gibbon, *Phys. Rev. Lett.* **76**, 50 (1996).
- [9] P. A. Norreys *et al.*, *Phys. Rev. Lett.* **76**, 1832 (1996).
- [10] J. Zhang *et al.*, *Phys. Rev. A* **54**, 1597 (1996).
- [11] J. D. Jackson, *Classical Electrodynamics* (Wiley, New York, 1975).
- [12] From Eq. (1) and the form of  $\vec{G}_n$ , it is easy to see that since  $\vec{\Delta}$  is field dependent, harmonics can be generated even if  $\vec{j}$  is linear in the fields. However, usually  $\vec{v}$  must be sufficiently large (nonlinear) to result in a finite  $\vec{\Delta}$ . We see also from Eq. (1) that although the latter does not alter significantly the magnitude of the radiation, it can greatly affect the angular distribution of the harmonics.
- [13] E. S. Sarachik and G. T. Schappert, *Phys. Rev. D* **1**, 2738 (1970).
- [14] The theory of scattering of a linearly polarized light and/or oblique incidence within the present model is considerably more involved, as the electron motion in the laser field has then an axial component. There is thus a finite-depth interaction layer. Nevertheless, if the latter is sufficiently thin, an effective surface current can still be constructed.